Triply charmed baryons mass decomposition from lattice QCD*

Jin-Bo Li (黎锦波)[1] Long-Cheng Gui (桂龙成)[1,2,3†] Wen Qin (秦文)[1,2,3‡]
Wei Sun (孙玮)[4§] Jian Liang (梁剑)[5,6¶]

[1]Department of Physics, Hunan Normal University, Changsha 410081, China
[2]Synergetic Innovation Center for Quantum Effects and Applications (SICQEA), Changsha 410081, China
[3]Key Laboratory of Low-Dimensional Quantum Structures and Quantum Control of Ministry of Education, Changsha 410081, China
[4]Institute of High Energy Physics, Chinese Academy of Sciences, Beijing 100049, China
[5]Key Laboratory of Atomic and Subatomic Structure and Quantum Control (MOE), Guangdong Basic Research Center of Excellence for Structure and Fundamental Interactions of Matter, Institute of Quantum Matter, South China Normal University, Guangzhou 510006, China
[6]Guangdong-Hong Kong Joint Laboratory of Quantum Matter, Guangdong Provincial Key Laboratory of Nuclear Science, Southern Nuclear Science Computing Center, South China Normal University, Guangzhou 51006, China

Abstract: We present the first calculation of the connected scalar matrix element and the momentum fraction of the charm quark within the $3/2^+$ and $3/2^-$ triply charmed baryons on lattice QCD. The results are based on overlap valence fermions on two ensembles of $N_f = 2+1$ domain wall fermion configurations with two lattice spacings. The corresponding sea quark pion masses are 300 MeV and 278 MeV. The separated contributions to the triply charmed baryon mass are derived through the decomposition of the QCD energy-momentum tensor. The contribution of the connected charm quark matrix element to the triply charmed baryon is about 3/2 times that of the charmonium, and it is almost 70% of the total mass. The mass splitting of $3/2^+$ and $3/2^-$ triply charmed baryons is mainly from the$\langle H_E \rangle$ of the QCD energy-momentum tensor. A mass decomposition based on the quark model is also studied for comparison.

Keywords: lattice QCD, triply charmed baryon, mass decomposition

DOI: 10.1088/1674-1137/adc0f4 **CSTR:** 32044.14.ChinesePhysicsC.49063103

I. INTRODUCTION

Since the discovery of the J/ψ meson in 1974 [1, 2], charm physics has garnered significant attention, leading to the identification of numerous charmed hadrons. Recently, the Large Hadron Collider (LHC) has made notable advancements in the study of charmed baryons, including the spectroscopy of excited hadrons such as Λ_c^+ [3], $\Omega_c(X)$ [4], and $\Xi_c(X)$ [5]. Notably, the doubly charmed baryon Ξ_{cc}^{++} was established by LHCb in 2017 [6] and has since been confirmed by subsequent studies [7, 8], following the initial identification of the charmed baryon Λ_c by Mark-II in 1979 [9]. However, the triply charmed baryon has yet to be observed experimentally, although some theoretical research indicates that it could be discovered at the LHC [10, 11].

Despite the lack of experimental evidence, theoretical investigations into the triply charmed baryon have been actively pursued using various approaches, including the quark model [12−18], QCD sum rules [19−21], Faddeev equations [22−24], the di-quark model [25, 26], the variational method [27, 28], the bag model [29, 30], Regge theory [31], and the Bethe-Salpeter equation [32]. These studies predict the mass of the ground state triply charmed baryon to be approximately 4.8 GeV. Numerous theoretical calculations have also been conducted to determine the mass spectrum under both quenched [33] and unquenched lattice QCD [34−44]. The predicted ground state mass from these lattice QCD calculations is consistent with other theoretical predictions.

Beyond spectroscopy, decomposing the mass of a

Received 29 December 2024; Accepted 13 March 2025; Published online 14 March 2025

* Supported by the National Natural Science Foundation of China (12175036, 11935017, 12175073, 12205311, 12222503), the Natural Science Foundation of Hunan Province, China (2023JJ30380, 2024JJ6300), the Department of Education Foundation of Hunan Province, China (20A310, 22B0044), and the Major Project of Basic and Applied Basic Research of Guangdong Province, China (2020B0301030008)

† E-mail: guilongcheng@hunnu.edu.cn
‡ E-mail: qinwen@hunnu.edu.cn
§ E-mail: sunwei@ihep.ac.cn
¶ E-mail: jianliang@scnu.edu.cn

hadron within the QCD framework offers deeper insights into its internal structure. This approach provides valuable information about the distribution of mass contributions from various components within the hadron. The mass decomposition of the nucleon was first proposed in [45], taking into account the dynamic interactions between quarks and gluons. In this framework, hadron mass is divided into four components: quark energy, quark mass, gluon energy, and trace anomaly. Mass decomposition has been explored in various hadronic systems, yielding novel insights [46−48]. For instance, it has been found that the trace anomaly contributes significantly in light hadron systems [46], and the quark mass matrix contributes less in hybrids compared to charmonium [48]. In this work, we aim to study the mass decomposition of the ground state triply charmed baryon using lattice QCD. We will first calculate the hadron mass M, the valence charm quark mass contribution $\langle H_m \rangle$, and the valence charm quark momentum fraction $\langle x \rangle_q$ using lattice QCD. Subsequently, the other components of the hadron mass can be determined through the decomposition formula of the QCD energy-momentum tensor (EMT) and the trace sum rule.

There is also a mass decomposition in the non-relativistic quark model, where the hadron mass is seperated into three parts: the mass and kinetic energy of the constituent quarks and the potential energy between them. The hyper-fine splitting is primarily attributed to the spin-spin interaction arising from the one-gluon exchange potential. Previous results for the heavy meson mass decomposition from lattice QCD appear to align with the perspective of the constituent quark model [46]. In this work, we also study the mass decomposition in the constituent quark model for comparison and attempt to gather clues of the correlation between the phenomenological model and QCD theory, which may deepen our understanding of their intrinsic nature. Because triply charmed baryons exist in an energy region where non-perturbative interactions cannot be ignored, a precise decomposition of the mass will provide valuable insights into comprehending the non-perturbative properties of QCD.

The remainder of our article is organized as follows: In Sec. II, we provide a detailed introduction to the hadron mass decomposition formula within the QCD framework. We also discuss the relationship between the hadron mass and two-point functions and between the hadron matrix elements and three-point functions. In Sec. III, we present details of our numerical simulations, including the configuration information, effective mass, effective matrix element calculations, and fitting results. In Sec. IV, we analyze and discuss our results, including comparisons with the constituent quark model. Finally, a brief summary is provided in Sec. V.

II. FORMALISM

A. Mass decomposition from the QCD EMT

In this article, we adopt the QCD energy-momentum tensor decomposition proposed by Ji [45] used in Refs. [46−48]. The QCD energy-momentum tensor is written as

$$T^{\mu\nu} = \frac{1}{2}\bar{\psi}\mathrm{i}\overleftrightarrow{D}^{(\mu}\gamma^{\nu)}\psi + \frac{1}{4}g^{\mu\nu}F^2 - F^{\mu\alpha}F^{\nu}_{\alpha}, \tag{1}$$

where () symmetrizes all the indices, $\overleftrightarrow{D}^{\mu} = \overrightarrow{D}^{\mu} - \overleftarrow{D}^{\mu}$, $\overrightarrow{D}$ is the gauge-covariant derivative, and $F^{\mu\nu}$ is the color field strength tensor. The QCD Hamiltonian and the hadron mass could be written in terms of the energy-momentum tensor

$$H_{\mathrm{QCD}} = \int \mathrm{d}^3x T^{00}(0,\mathbf{x}), \tag{2}$$

$$M = \frac{\langle H|H_{\mathrm{QCD}}|H\rangle}{\langle H|H\rangle} \equiv \langle T^{00}\rangle,$$

where the hadron state $|H\rangle$ is renormalized as $\langle H|H\rangle = 2E(2\pi)^3\delta^3(0)$.

The hadron mass can be decomposed as

$$M = \langle T^{00}\rangle = \langle H_M\rangle + \langle H_E^{(\mu)}\rangle + \langle H_g^{(\mu)}\rangle + \frac{1}{4}\langle H_a\rangle \tag{3}$$

in the rest frame of the hadron state with

$$H_E^{(\mu)} = \sum_f \int \mathrm{d}^3x \bar{\psi}^{(f)}(\vec{D}\cdot\vec{\gamma})\psi^{(f)}, \tag{4}$$

$$H_M = \sum_f \int \mathrm{d}^3x \bar{\psi}^{(f)} m_f \psi^{(f)}, \tag{5}$$

$$H_g^{(\mu)} = \int \mathrm{d}^3x \frac{1}{2}(B^2 - E^2), \tag{6}$$

$$H_a = \int \mathrm{d}^3x \left[\gamma_m \sum_f \bar{\psi}^{(f)} m_f \psi^{(f)} - \frac{\beta(g)}{g}(B^2 + E^2)\right], \tag{7}$$

where $\sum_f$ denotes the summation of quark flavors, γ_m is the quark mass anomalous dimension, and $\beta(g)$ is the QCD β function. H_E, H_M, H_g, and H_a denote contributions from the quark energy, quark condensate, gluon field energy, and joint contributions to quantum anomalies from gluons and quarks in Euclidean space, respectively. Both $\langle H_M\rangle$ and $\langle H_a\rangle$ are independent of scale and

renormalization scheme. In contrast, the quark energy $\langle H_E^{(\mu)}\rangle$ and gluon field energy $\langle H_g^{(\mu)}\rangle$ are scale and renormalization dependent.

Thus, the renormalized quark and gluon energy are derived as

$$\langle H_E^R\rangle = \frac{3}{4}\langle x\rangle_q^R M - \frac{3}{4}\langle H_M\rangle, \quad \langle H_g^R\rangle = \frac{3}{4}\langle x\rangle_g^R M, \tag{8}$$

where $\langle x\rangle_q^R$ and $\langle x\rangle_g^R$ are the renormalized momentum fractions of quarks and gluons, respectively. These fractions satisfy the relation $\langle x\rangle_g^R = 1 - \langle x\rangle_q^R$ [49]. Following Ref. [48], we could also define the total valence charm quark contribution as

$$\langle H_q^R\rangle = \langle H_E^R\rangle + \langle H_M\rangle = \frac{3}{4}\langle x\rangle_q^R M + \frac{1}{4}\langle H_M\rangle. \tag{9}$$

In combination with the trace sum rule [50]

$$M = \langle T_\mu^\mu\rangle = \langle H_M\rangle + \langle H_a\rangle, \tag{10}$$

a component of the mass decomposition will be obtained through the calculation of the hadron mass M, the quark condensate contribution $\langle H_M\rangle$, and the quark energy contribution $\langle H_E\rangle$.

B. Two-point and three-point functions

The components of the mass decomposition can be extracted from the corresponding two-point and three-point correlation functions. To construct the correlation function for the triply charmed baryon, similar to the Omega baryon [51], we use the operator for the triply charmed baryon as

$$O_\gamma^\mu(\vec{x},t) = \epsilon^{abc}[\psi_\alpha^a(\vec{x},t)^T(C\gamma^\mu)_{\alpha\beta}\psi_\beta^b(\vec{x},t)]\psi_\gamma^c(\vec{x},t), \tag{11}$$

where $C = \gamma_2\gamma_4$ is the C-parity operator; α, β, γ represent the Dirac indices; a, b, and c are the color indices; and T is the transpose operator. To project onto a definite parity, we use the following parity projection operator:

$$P_\pm = \frac{1}{2}(1 \pm \gamma_4). \tag{12}$$

Additionally, to project onto the triply charmed baryon with a definite spin, we use the following spin projection operators [52]:

$$\begin{cases} P_{\frac{3}{2}}^{\mu\nu} = \delta^{\mu\nu} - \frac{1}{3}\gamma^\mu\gamma^\nu, \\ P_{\frac{1}{2}}^{\mu\nu} = \frac{1}{3}\gamma^\mu\gamma^\nu. \end{cases} \tag{13}$$

In our study, only the spatial components of the triply charmed baryon operator are considered. Therefore, the baryon operator with a definite J^P quantum number can be expressed as

$$O^i(\vec{x},t) = (P_\pm)_{\rho\rho'} \times \sum_j (P_J)_{\rho'\gamma}^{ij}\epsilon^{abc}\left[\psi_\alpha^a(\vec{x},t)^T(C\gamma^j)_{\alpha\beta}\psi_\beta^b(\vec{x},t)\right]\psi_\gamma^c(\vec{x},t). \tag{14}$$

The hadron mass M can be obtained from the two-point correlation function

$$C_2(t) = \sum_{\vec{x}}\langle O(\vec{x},t)O^\dagger(\vec{0},0)\rangle = \sum_n Z_n^2 e^{-M_n t} \xrightarrow{t\to\infty} Z_0^2 e^{-M_0 t}, \tag{15}$$

here, M_0 represents the ground state hadron mass, and Z_0 is the overlap matrix element between the ground state hadron and the hadron operator. Hadronic matrix elements, such as the quark content $\langle H_M\rangle$ and the quark momentum fraction $\langle x\rangle_q$, can be extracted from the three-point function

$$C_3(t,t',J,\hat{O}) = \sum_{\vec{x},\vec{y},t'}\langle O(\vec{x},t)J(\vec{y},t')O^\dagger(\vec{0},0)\rangle, \xrightarrow{t\gg t'\gg 0, t\to\infty} Z_0^2 e^{-M_0 t}\langle\Omega_{ccc}|J(\vec{0})|\Omega_{ccc}\rangle, \tag{16}$$

where $J(\vec{y},t')$ refers to the current operator. Here, we only considered the contribution of the valence charm quark. For the quark content $\langle H_m\rangle$, the corresponding current operator is

$$\hat{H}_M(\vec{y},t') = m_c\bar{\psi}^{(c)}(\vec{y},t')\psi^{(c)}(\vec{y},t'), \tag{17}$$

where m_c refers to the bare charm quark mass. For the charm quark momentum fraction $\langle x\rangle_q$, the current operator is

$$\hat{x}_q(\vec{y},t') = \frac{1}{2}\bar{\psi}^{(c)}(\vec{y},t')(\gamma_4\overleftrightarrow{D}_4 - \frac{1}{3}\gamma_i\overleftrightarrow{D}_i)\psi^{(c)}(\vec{y},t'). \tag{18}$$

III. NUMERICAL DETAILS

In this calculation, we used the 2+1 flavor domain wall fermion and Iwasaki gauge action configurations provided by the RBC/UKQCD collaboration [53, 54]. Table 1 presents the parameters of these gauge ensembles. For the valence charm quark, we employ the overlap fermion with exact chiral symmetry on the lattice, which ensures that the valence charm quark mass matrix $\langle H_M\rangle$ is independent of the renormalization scale and scheme [55]. The valence charm quark mass adopted in both ensembles follows the same tuning procedure as in

Table 1. The parameters for the configurations [48].

Ensemble	$L^3\times T$	a/fm	m_π/MeV	$m_c a$	$N_{\rm cfg}$
32I	$32^3\times 64$	0.0828(3)	300	0.493	305
48If	$48^3\times 96$	0.0711(3)	278	0.410	205

Ref. [48], where the physical J/ψ mass was used as the matching criterion.

To extract the hadron mass, we directly fit the two-point correlation function. Considering the unphysical oscillatory behavior introduced by the Domain Wall fermion [56], we use the following fitting function for the two-point function:

$$C_2(t) = A_0 \mathrm{e}^{-Mt}\left(1 + A_1 \mathrm{e}^{-\delta m t}\right) + W(-1)^t \mathrm{e}^{-\widetilde{M}t}. \tag{19}$$

In this expression, $\mathrm{e}^{-\delta m t}$ is used to absorb the contributions from the excited states, and $\mathrm{e}^{-\widetilde{M}t}$ is the oscillating term. The parameters M, δm, $\widetilde{M}$, W, A_0, and A_1 are determined through the fitting process. This approach allows us to account for and mitigate the effects of oscillations in the data when determining the hadron mass.

The effective masses of the two triply charmed baryons with quantum numbers $J^P = 3/2^+$ and $J^P = 3/2^-$ obtained from two different lattice configurations are depicted in Fig. 1. In the figure, the dark color bands represent our fitting range, while the light color bands indicate the extrapolation results. The fitted masses and δm of the two different triply charmed baryons are shown in Table 2. Because we have two lattice spacings and the results on the two ensembles are consistent within errors, we perform a constant extrapolation to obtain the results at the continuum limit.

To obtain the charmness content $\langle H_M\rangle$ and the charm quark momentum fraction $\langle x\rangle_q$, we must calculate the corresponding three-point correlation functions. We employ the Feynman-Hellmann inspired method to compute the three-point function as done in Refs. [48, 57] and readers are referred to Ref. [58] for more details. The corresponding current-summed three-point function is given by

$$\begin{aligned} C^{(3)}(t,J,O) &= \sum_{t'=0}^{T-1}\langle 0|T\left\{O(t)\mathcal{J}(t')O^\dagger(0)\right\}|0\rangle \\ &= \sum_{y,c}\langle \Gamma G_c^J(\vec{y},t;0)G(\vec{y},t;0)G(\vec{y},t;0)\rangle, \\ &= \sum_{t'=1}^{t-1}\sum_{n,m}\langle 0|O(t)|n\rangle\langle n|\mathcal{J}(t')|m\rangle\langle m|O^\dagger(0)|0\rangle \\ &+II+III+VI = \sum_n\left[(t-1)Z_nJ_{nn}Z_n^\dagger + d_n\right] \\ &\times \mathrm{e}^{-E_n t} + \sum_{n\neq m} Z_nJ_{nm}Z_m^\dagger \frac{\mathrm{e}^{-E_n t}\mathrm{e}^{\frac{\Delta_{nm}}{2}} - \mathrm{e}^{-E_m t}\mathrm{e}^{\frac{\Delta_{nm}}{2}}}{\mathrm{e}^{\frac{\Delta_{nm}}{2}} - \mathrm{e}^{\frac{\Delta_{nm}}{2}}}. \end{aligned} \tag{20}$$

Here, the sum over c represents the various possible con-

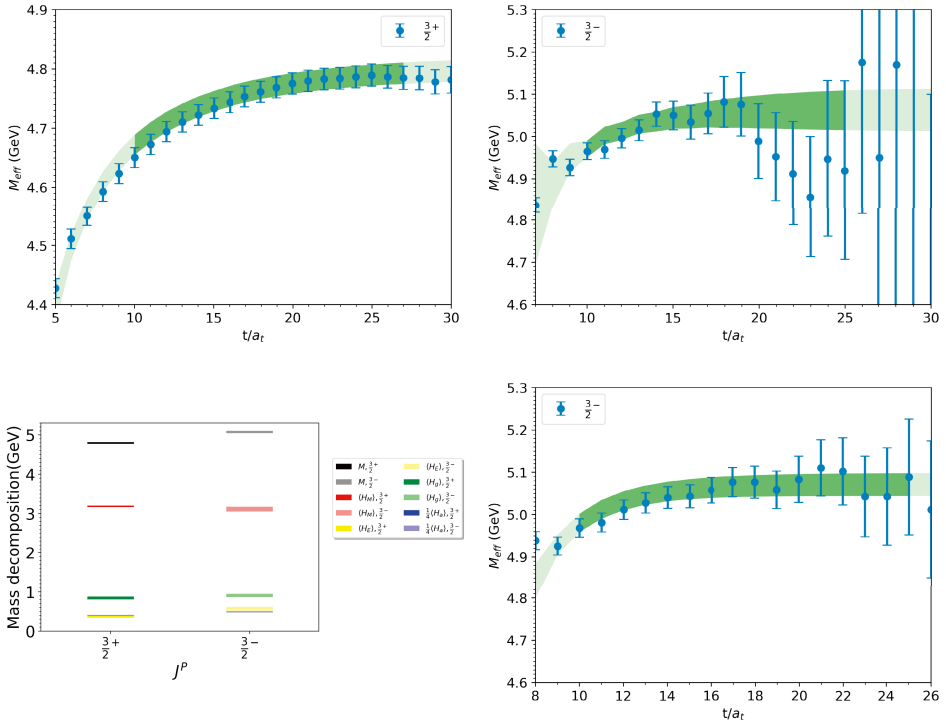

Fig. 1. (color online) Effective mass $m_{\rm eff} = \ln\left(\frac{C_2(t+1)}{C_2(t)}\right)$ for two triply charmed baryon states on $32^3\times 64$ (top) and $48^3\times 96$ (bottom) configurations.

Table 2. The hadron mass for two triply charmed baryon states on $32^3\times64$ (32I) and $48^3\times96$ (48If) configurations along with the fitting range $[t_{\rm min}-t_{\rm max}]$ and χ^2/d.o.f. The results of constant extrapolation are also shown in the last row.

Ensemble	J^P	M/GeV	δm/GeV	$[t_{\rm min}-t_{\rm max}]$	χ^2/d.o.f
32I	$\frac{3}{2}^+$	4.804(20)	0.300(52)	10−27	0.76
	$\frac{3}{2}^-$	5.064(51)	0.64(64)	10−25	1.4
48If	$\frac{3}{2}^+$	4.793(21)	0.439(58)	13−38	0.42
	$\frac{3}{2}^-$	5.071(27)	1.14(36)	10−25	0.85
∞	$\frac{3}{2}^+$	4.799(14)			
	$\frac{3}{2}^-$	5.069(24)			

tractions of the current coupling to a quark propagator and G_c^J denotes the Feynman-Hellmann propagator

$$G_c^J(\vec{y},t;0)=\sum_{\vec{x},t'}G(\vec{y},t;\vec{x},t')J(\vec{x},t')G(\vec{x},t';0). \tag{21}$$

Γ represents the product of the initial and final state γ matrices. For simplicity, the contraction over color indices is omitted. II, III, and IV denote the contributions from the regions of $t<t'<T$, $t'=0$, and $t'=t$, respectively, and they are absorbed in the d_n term despite a e^{-E_nt} factor. Z_n represents the overlap factor. J_{nn} denotes the hadronic matrix element. Δ_{nm} is defined as $\Delta_{nm}\equiv E_m-E_n$.

The ratio of the three-point function to the corresponding two-point function is defined as

$$R(t)=\frac{C^{(3)}(t)}{C^{(2)}(t)}\simeq(t-1)J_{00}+\frac{d_n}{|Z_0|^2}+J_{10}\frac{Z_1}{Z_0}\frac{e^{\frac{\Delta_{10}}{2}}}{e^{\frac{\Delta_{10}}{2}}-e^{\frac{\Delta_{01}}{2}}}+\sum_{n=1}C_n(t-1)e^{-\Delta_{n0}t}+D_ne^{-\Delta_{n0}t}. \tag{22}$$

In the second step, we assume that $C^{(2)}(t)$ is primarily contributed by the ground state and incorporate some of the coefficients related to the excited states into C_n and D_n for simplicity. We can derive the matrix element J_{00} from the derivative of $R(t)$

$$\partial_tR(t)\equiv R(t-1)-R(t)\xrightarrow{t\to\infty}J_{00}. \tag{23}$$

Although the subtraction procedure may introduce larger relative statistical uncertainties, it efficiently generates results for multiple all sink times. It avoids the computational cost of repeatedly calculating propagators for each sink time (as in traditional sink-sequential approaches). The increased data density across time separations improves the control of excited-state contamination and enhances the accuracy of extracting the desired hadronic matrix elements. The lattice correlator with all sink times available improves the control of excited-state contamination (at sink) and thus the extraction of the desired matrix elements. The final numerical results are all of decent precision.

The effective hadronic matrix elements can be obtained from the difference of $R(t)$ as

$$\begin{aligned}\langle H_M\rangle(t)&=R(t,\hat{H}_M,\hat{Q})-R(t-1,\hat{H}_M,\hat{Q}),\\ M\langle x\rangle_q(t)&=R(t,\hat{x},\hat{Q})-R(t-1,\hat{x},\hat{Q}).\end{aligned} \tag{24}$$

Then, the hadronic matrix elements $\langle H_M\rangle$ and $M\langle x_q\rangle$ can be fitted using the formulas as

$$\begin{aligned}\langle H_M\rangle(t)&=\langle H_M\rangle+A_1'e^{-\delta mt}+tA_2'e^{-\delta mt},\\ M\langle x_q\rangle(t)&=M\langle x_q\rangle+A_3'e^{-\delta mt}+tA_4'e^{-\delta mt},\end{aligned} \tag{25}$$

where δm, H_M, x_q, A_1', A_2', A_3', and A_4' are fitting parameters, and the exponential terms are used to absorb the contribution from excited states.

The fitting of the effective matrix elements of the charmness content $\langle H_M\rangle$ and the valence charmed quark momentum fraction $\langle x\rangle_q$ are shown in Fig. 2 and Fig. 3, respectively. The dark color bands represent our fitting range, while the light color bands show the extrapolation results. The fitted results of the corresponding hadron matrix elements are shown in Table 3 and Table 4. Our results reveal that, on two different configurations, the charmness content of the orbital excited state $3/2^-$ is slightly smaller than that of the ground state $3/2^+$.

IV. DISCUSSION

A. Mass spectrum

Before delving into the mass decomposition of the triply charmed baryon, we first briefly review and discuss the mass spectrum. Numerous lattice QCD studies have been conducted on the spectrum, and we have compiled their results alongside ours in Table 5, which are also presented more intuitively in Fig. 4. Regarding the ground $3/2^+$ state, most of the results are in good agreement. The result of Ref. [42] is as low as 4.6769(46)(30).

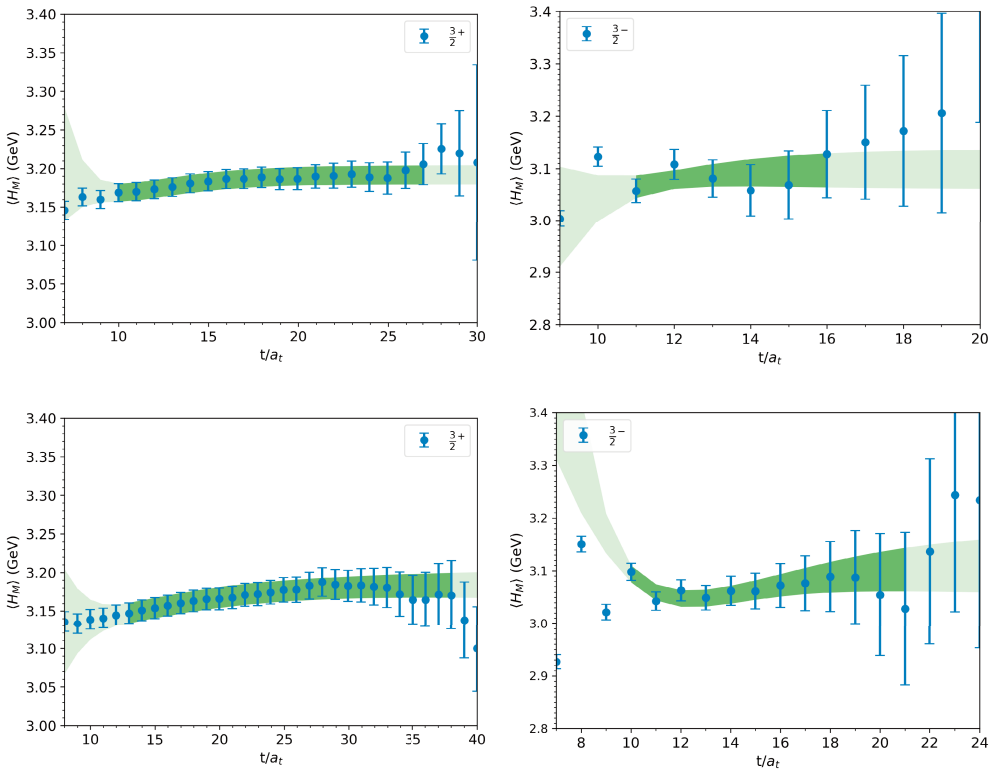

Fig. 2. (color online) Effective matrix elements of the charmness content $\langle H_M \rangle$ for two triply charmed baryon states on $32^3 \times 64$ (top) and $48^3 \times 96$ (bottom) configurations.

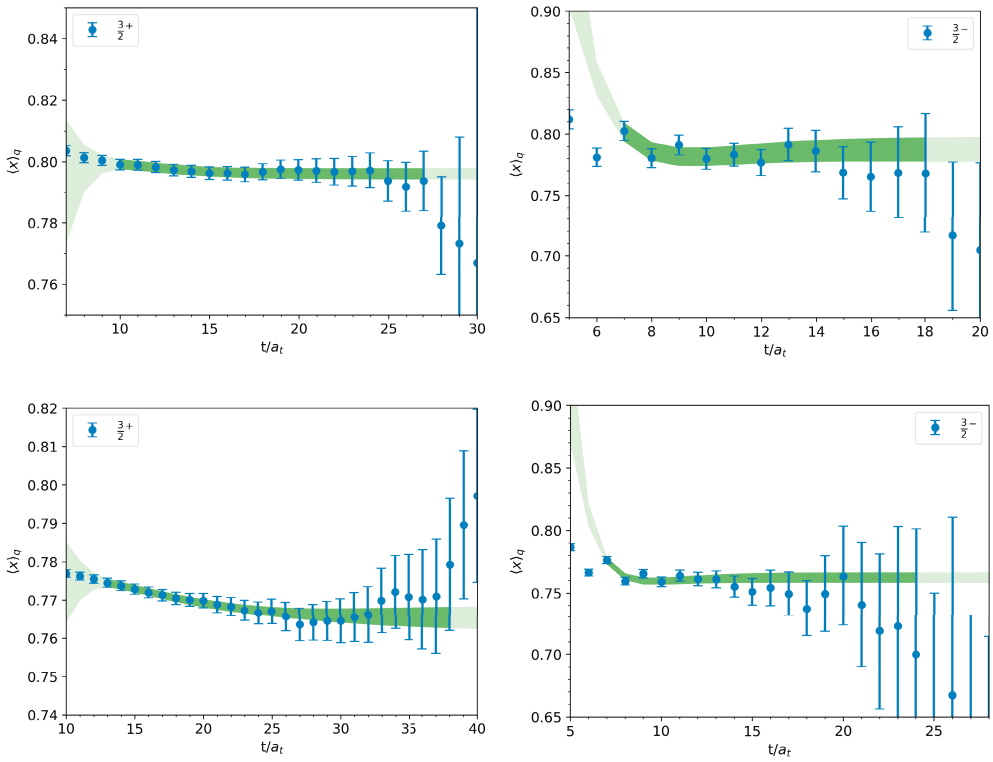

Fig. 3. (color online) Effective matrix elements of valence charmed quark momentum fraction $\langle x \rangle_q$ for two triply charmed baryon states on $32^3 \times 64$ (top) and $48^3 \times 96$ (bottom) configurations.

Table 3. The charmness content $\langle H_M \rangle$ for two triply charmed baryon states on $32^3\times64$ (top) and $48^3\times96$ (bottom) configurations along with the corresponding fitting range $[t_{\rm min}-t_{\rm max}]$ and χ^2/d.o.f.

Ensemble	J^P	$\langle H_M\rangle$/GeV	$[t_{\rm min}-t_{\rm max}]$	χ^2/d.o.f
32I	$\frac{3}{2}^+$	3.192(13)	10−27	0.062
	$\frac{3}{2}^-$	3.098(38)	11−16	0.38
48If	$\frac{3}{2}^+$	3.185(19)	13−38	0.089
	$\frac{3}{2}^-$	3.114(60)	10−21	0.33

Table 4. The charmed quark momentum fraction $\langle x\rangle_q$ for two triply states on $32^3\times64$ (top) and $48^3\times96$ (bottom) configurations along with the corresponding fitting range $[t_{\rm min}-t_{\rm max}]$ and χ^2/d.o.f.

Ensemble	J^P	$\langle x\rangle_q$	$[t_{\rm min}-t_{\rm max}]$	χ^2/d.o.f
32I	$\frac{3}{2}^+$	0.7960(18)	10−27	0.096
	$\frac{3}{2}^-$	0.7878(99)	7−18	1.7
48If	$\frac{3}{2}^+$	0.7653(33)	13−38	0.12
	$\frac{3}{2}^-$	0.7623(42)	7−24	1.1

However, the result is updated to 4.746(4)(32) when simulations were performed on configurations with the physical pion mass in Ref. [41]. Our results for the $3/2^+$ state are consistent with the other lattice calculations within error bars. For the p-wave $3/2^-$ state, the corresponding lattice calculations are fewer, and the uncertainties are relatively larger. Our results align closely with those of the TRJQCD collaboration but are slightly smaller than the results from the HSC and TWQCD collaborations. Considering that TRJQCD performed simulations on configurations close to the physical pion mass, the results we obtained here appear reasonable. After our work, two recent studies have also calculated the masses of the triply charmed baryon [59, 60]. In summary, the mass spectrum we obtained is consistent with other lattice calculations, indicating the reliability of our results within current computational constraints.

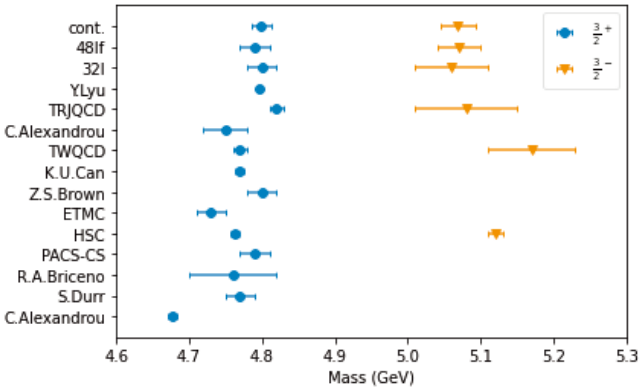

Fig. 4. (color online) Masses of $3/2^+$ and $3/2^-$ triply charmed baryons on lattice QCD.

B. Mass decomposition

Table 5. The masses of the ground state $\Omega_{ccc}(1^4S_{3/2^+})$ and the orbital excited state $\Omega_{ccc}(1^2P_{3/2^-})$we calculated on $32^3\times64$ (48If) and $48^3\times96$ (32I) configurations are shown alongside the results from other lattice QCD collaborations. The corresponding flavor number (N_f), lattice spacings (a), pion mass (m_π), actions of relevant sea ($S_q^{\rm sea}$), and valence charm ($S_c^{\rm val}$) quarks are included for comparison. The abbreviations HISQ and RHQA stand for highly-improved staggered quark and relativistic heavy-quark action, respectively.

Collaboration	N_f	a/fm	m_π/GeV	$S_q^{\rm sea}$	$S_c^{\rm val}$	$\Omega_{ccc}(\frac{3}{2}^+)$/GeV	$\Omega_{ccc}(\frac{3}{2}^-)$/GeV
[Ours]48If	2+1	0.0711(3)	0.278	Domain-wall	Overlap	4.793(21)	5.071(27)
[Ours]32I	2+1	0.0828(3)	0.3	Domain-wall	Overlap	4.804(20)	5.064(51)
[Ours]continuum	2+1					4.799(14)	5.069(24)
Y.Lyu *et al.* [61]	2+1	0.0846	0.146	Wilson	RHQA	4.7956(7)	
TRJQCD [40]	2+1	0.0907(13)	0.156(9)	Clover	Clover	4.817(12)	5.083(67)
C.Alexandrou *et al.* [41]	2	0.0938(3)(2)	0.130	Twisted Mass	OS	4.746(4)(32)	–
TWQCD [44]	2+1+1	0.063	0.280	Domain-wall	Domain-wall	4.766(5)(11)	5.168(37)(51)
K.U.Can [38]	2+1	0.0907(13)	0.156(7)(2)	Wilson	Clover	4.769(6)	–
Z.S.Brown *et al.* [37]	2+1	0.085−0.11	0.227−0.419	Domain-wall	RHQA	4.796(8)(18)	–
ETMC [39]	2+1+1	0.065−0.094	0.210−0.430	Twisted Mass	Twisted Mass	4.734(12)(11)(9)	–
HSC [36]	2+1	0.0351(2)	0.390	Clover	Clover	4.763(6)	5.124(13)
PACS-CS [35]	2+1	0.0899	0.135(6)	Clover	RHQA	4.789(22)	–
R.A.Briceno *et al.* [34]	2+1+1	0.06−0.12	0.220−0.310	HISQ	RHQA	4.761(52)(21)(6)	–
S.Durr *et al.* [43]	2	0.0728(5)(19)	0.280	Wilson	Brillouin	4.774(24)	–
C.Alexandrou *et al.* [42]	2	0.0561(1)−0.089(1)	0.260−0.450	Twisted Mass	OS	4.6769(46)(30)	–

This study neglected the sea charm quark mass term $\langle H_M^{c,\mathrm{sea}}\rangle$ for calculation convenience. This is a reasonable approximation since $\langle H_M^{c,\mathrm{sea}}\rangle$ is estimated to be less than 100 MeV for both $3/2^+$ and $3/2^-$ states on each lattice ensemble based on the heavy quark expansion [50]:

$$\langle H_M^{c,\mathrm{sea}}\rangle = \frac{2}{27}\left(\frac{1}{1+\gamma_m(\mu)}M - \langle H_M^{c,v}\rangle\right) + O(\alpha_s). \tag{26}$$

Here, $\gamma_m(\mu) \approx \dfrac{2\alpha(\mu)}{\pi}$ is the quark anomalous dimension and $\alpha(\mu = m_c) \approx 0.37$ is taken from Ref. [62]. As to the light and strange sea quarks, we conjecture that it is also safe to neglect their contributions, based on the observation that their total contribution is less than 40 MeV in charmonium [48]. Disconnected diagrams are also not considered, so their contribution is absorbed in the QCD anomaly term H_a and the gluon energy term H_g. Possibly this is the reason why the values of H_a and H_g we obtained in the triply charmed baryon are slightly larger than those in charmonium states, as shown in Table 6 and more intuitively illustrated in Fig. 5. Nevertheless, the total valence charm quark contribution H_q remains the main contributor to the triply charmed baryon mass, accounting for approximately 75% of the total mass. This is consistent with the pattern observed in charmonium but differs from that in light baryons, where the trace anomaly contribution is more significant.

The quark mass contribution H_M in the triply charmed baryon is about 3/2 times that in charmonium. This is consistent with the scenario where a baryon is composed of three valence quarks while a meson is composed of two. In fact, the quark condensate contribution is similar to the well-known sigma term in nucleon physics. Following the definition of the sigma term, we define the renormalized charmness matrix element in the triply charmed baryon as

$$\mathcal{M}_S \equiv \langle \Omega_{ccc}(\vec{k}=0)|Z_S\bar{\psi}^c\psi^c|\Omega_{ccc}(\vec{k}=0)\rangle, \tag{27}$$

where Z_S is the renormalization constant of the scalar current. As done in Refs. [63, 64], we adopt Z_S = [1.009(16), 1.008(26)] for the ensembles of 32I and 48If, respectively. The charmness matrix element for the triply charmed baryon $3/2^+$ and $3/2^-$ states are obtained as shown in Table 6, where they are shown alongside those of the charmonium. The charmness matrix elements in triply charmed baryons are greater than those in charmonium. This difference arises primarily because the scalar current operator couples to the triply charmed baryon with a factor of 3, whereas the corresponding factor for charmonium is 2. If the effects of these factors are removed, the relation $\frac{1}{3}\mathcal{M}_S(\Omega) \sim \frac{1}{2}\mathcal{M}_S(\bar{c}c) \sim 0.9$ is obtained.

Moreover, the mass decomposition provides insights into the nature of the mass splitting between s-wave ($3/2^+$) and the p-wave ($3/2^-$) states. Our calculations indicate a mass splitting of approximately 250 MeV, with the primary contribution stemming from the quark energy term at around 200 MeV. In contrast, the contributions from the QCD anomaly term H_a and the gluon energy term H_g are each less than 100 MeV. This differs from the scenario in charmonium, where the contributions of H_g and H_a are comparable to that of H_E, as shown in the charmonium mass decompositions in Table 6. For comparison, we have also calculated the rest energy composition of the ground state ($3/2^+$) and orbitally excited state ($3/2^-$) triply charmed baryons within the framework of the constituent quark model. Following Ref. [16], the Hamiltonian for the triply charmed baryon can be expressed as

$$H = M_q + T + \sum_{i,j;i<j}^{3} V_{ij}^C + V_{ij}^G, \tag{28}$$

where M_q and T denote the mass and kinetic energy of the constituent quarks, respectively. V_{ij}^C is the confinement potential defined as $V_{ij}^C = \dfrac{b}{2}r_{ij}$. V_{ij}^G is the one-gluon

Table 6. Mass decomposition of $3/2^+$ and $3/2^-$ triply charmed baryon states on $32^3\times64$ (top) and $48^3\times96$ (bottom) configurations, along with the mass decomposition of charmonium states. The charmness matrix element $\mathcal{M}_s$ are also listed for comparison.

J^P	M/GeV	$\langle H_M\rangle$/GeV	$\langle H_E\rangle$/GeV	$\langle H_g\rangle$/GeV	$\frac{1}{4}\langle H_a\rangle$/GeV	$\mathcal{M}_S$
$\frac{3}{2}^+$	4.804(20)	3.192(13)	0.474(17)	0.735(30)	0.403(06)	2.742(46)
$\frac{3}{2}^-$	5.064(51)	3.098(38)	0.669(56)	0.806(86)	0.492(16)	2.661(54)
J/ψ	3.104(02)	2.162(02)	0.264(03)	0.442(02)	0.2355(07)	1.857(30)
χ_{c1}	3.434(11)	2.101(30)	0.335(37)	0.664(28)	0.333(08)	1.805(39)
$\frac{3}{2}^+$	4.793(21)	3.185(19)	0.362(22)	0.844(37)	0.402(07)	2.822(76)
$\frac{3}{2}^-$	5.071(27)	3.114(60)	0.564(50)	0.904(84)	0.489(16)	2.759(90)
J/ψ	3.100(01)	2.139(01)	0.2116(25)	0.509(02)	0.2403(04)	1.895(50)
χ_{c1}	3.480(18)	2.063(38)	0.387(47)	0.676(37)	0.354(11)	1.828(58)

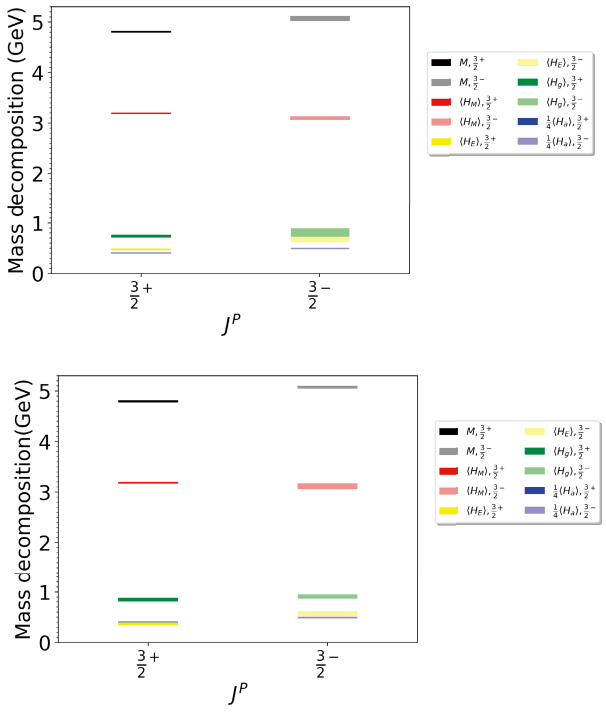

Fig. 5. (color online) Mass decomposition for of $3/2^+$ and $3/2^-$ triply charmed baryon states on $32^3\times64$ (top) and $48^3\times96$ (bottom) configurations.

exchange potential, and the explicit expression along with the quantities involved are written as follows:

$$V_{ij}^{G} = V_{ij}^{\text{coul}} + V_{ij}^{sd}, \tag{29}$$

$$V_{ij}^{\text{coul}} = -\frac{2}{3}\frac{\alpha_{ij}}{r_{ij}}, \tag{30}$$

$$V_{ij}^{sd} = V_{ij}^{SS} + V_{ij}^{T} + V_{ij}^{LS}, \tag{31}$$

$$V_{ij}^{SS} = -\frac{2\alpha_{ij}}{3}\left\{-\frac{\pi}{2}\cdot\frac{\sigma_{ij}^3 \mathrm{e}^{-\sigma_{ij}^2 r_{ij}^2}}{\pi^{3/2}}\cdot\frac{16}{3m_c^2}\left(\mathbf{S}_i\cdot\mathbf{S}_j\right)\right\}, \tag{32}$$

$$V_{ij}^{T} = \frac{2\alpha_{ij}}{3}\cdot\frac{1}{m_c^2 r_{ij}^3}\left\{\frac{3\left(\mathbf{S}_i\cdot\mathbf{r}_{ij}\right)\left(\mathbf{S}_j\cdot\mathbf{r}_{ij}\right)}{r_{ij}^2} - \mathbf{S}_i\cdot\mathbf{S}_j\right\}, \tag{33}$$

$$V_{ij}^{LS} = \frac{\alpha_{\text{SO}}}{\rho^2+\lambda^2}\cdot\frac{\mathbf{L}\cdot\mathbf{S}}{27m_c^2}. \tag{34}$$

Here, S_i, S, and L are the spin operator of the i-th quark, the total spin of the baryon, and the total orbital angular momentum of the baryon, respectively. b, α_{ij}, and α_{SO} denote the strength of confinement potential, strong coupling, and spin-orbit potential. The same parameters are adopted as in Ref. [16]. The corresponding mass decomposition with explicit values of M_q, T, V^C, V^{coul}, V^{SS}, V^T ,and V^{SL} for both the $3/2^+$ and $3/2^-$ states are derived as shown in Table 7.

The constituent quark mass terms for the $3/2^+$ and $3/2^-$ states are identical, each being three times the constituent quark mass. Notice that the constituent quark mass is input as a constant, and the kinetic energy terms are similar for both states. The mass difference between the $3/2^+$ and $3/2^-$ states primarily arises from the potential energy terms V^C and V^G. The influences of these two potential terms act in opposite directions. The confinement potential V^C has a constructive effect on hadron mass, while the one-gluon exchange potential V^G exerts a destructive influence. The $3/2^-$ state has a stronger confinement potential coupled with a weaker one-gluon exchange potential, leading to a slightly higher mass compared to the $3/2^+$ state, which is consistent with lattice QCD calculations.

It is quite complicated to directly relate lattice QCD to phenomenological models. However, under certain limits, quantities defined in lattice QCD can reflect phenomenological insights. For example, the gluon trace anomaly term $\langle H_a^g\rangle$ for a heavy quark-antiquark pair system is related to the confinement potential by

$$\langle H_a^g\rangle_{\bar{c}c} = A + 2\langle V(r)\rangle, \tag{35}$$

in the heavy quark limit, as demonstrated in Refs. [65, 66]. Here, A is a constant and $V(r)=\sigma r$ is the confinement potential. One may wonder whether this relation still holds for triply charmed baryons. In our calculation, the gluon trace anomaly term $\langle H_a^g\rangle_H = \langle\frac{\beta}{2g}\int \mathrm{d}^3\vec{x}G^2\rangle_H$ can be deduced from

$$\langle H_a^g\rangle_H = \langle H_a\rangle_H - \langle H_a^q\rangle_H, \tag{36}$$

where $\langle H_a^q\rangle_H = \gamma_m\langle H_m\rangle_H$ denotes the quark trace anomaly term. Here, we focus on the difference in $\langle H_a^g\rangle_H$ for the $3/2^+$ and $3/2^-$ states to eliminate the effect of the unknown constant A. Adopting $\gamma_m = 0.295$ from Ref. [60], we find that the difference of the gluon trace anomaly term is $\Delta\langle H_a^g\rangle_{\Omega_{ccc}} \equiv \langle H_a^g\rangle_{\frac{3}{2}^-} - \langle H_a^g\rangle_{\frac{3}{2}^+} = 0.384(69)_{32\text{I}}$ GeV or $0.369(72)_{48\text{IF}}$ GeV. In comparison, the corresponding difference of the confinement potential in the quark model is $\Delta V^C(r) \equiv V^C(r)_{\frac{3}{2}^-} - V^C(r)_{\frac{3}{2}^+} \simeq 0.16$ GeV. This approximately satisfies the relation $\Delta\langle H_a^g\rangle_{\Omega_{ccc}} \simeq 2\Delta\langle V^C\rangle$, which is consistent with the charmonium case in the heavy quark limit as denoted by Eq. (35). It implies that there may be a connection between the trace anomaly and hadron confinement. Further studies on this issue would be benefi-

Table 7. Mass decomposition in the quark model. M is the hadron mass of a triply charmed baryon. M_q represents the quark mass term, T denotes the kinetic energy term, V^C stands for the confinement potential, $V^{\rm coul}$ is the Coulomb potential, V^{SS} refers to the spin-spin potential, and V^{LS} is the spin-orbit potential. The tensor potential V^T is zero in both of these states and has therefore been excluded. The data are given in MeV.

J^P	M	M_q	T	V^C	$V^{\rm coul}$	V^{SS}	V^{LS}
$\frac{3}{2}^+$	4828	4450	533	471	−647	21	0
$\frac{3}{2}^-$	5162	4450	538	630	−466	4	7

cial.

V. SUMMARY

This study investigated the mass decomposition of triply charmed baryons within the lattice QCD framework. The two lowest triply charmed baryons were calculated on two lattice ensembles, and an appropriate mass spectrum that was consistant with other calculations was obtained. The mass decompositions of both $3/2^+$ and $3/2^-$ triply charmed baryon states on two lattices were obtained. We found that the total valence charm quark contribution H_q is dominant in triply charmed baryon, which is consistent with the pattern observed in charmonium but differs from that displayed in nucleons, where the trace anomaly contribution plays a major role.

We also calculated the mass decomposition of these two states in the constituent quark model. It is challenging to directly correlate the mass components decomposed on lattice QCD with those in the quark model. Nevertheless, an analysis of the gluon trace anomaly in triply charmed baryons demonstrated a relation with the confinement potential analogous to that of the heavy quark-antiquark system. This implies a possible connection between the trace anomaly and the confinement potential.

ACKNOWLEDGEMENT

The authors L. C. Gui, W. Sun and J. Liang, as memebers of the χQCD corllaboration, thank the RBC collaboration for providing us their DWF gauge configurations. We thank Hui-hua Zhong for useful discussion. The computations were performed on the Xiangjiang-1 cluster at Hunan Normal University (Changsha) and the Southern Nuclear Science Computing Center (SNSC) and the HPC clusters at Institute of High Energy Physics (Beijing) and China Spallation Neutron Source (Dongguan) and the ORISE Supercomputer.

References

[1] J. J. Aubert *et al.* (E598), Phys. Rev. Lett. **33**, 1404 (1974)
[2] J. E. Augustin *et al.* (SLAC-SP-017), Phys. Rev. Lett. **33**, 1406 (1974)
[3] R. Aaij *et al.* (LHCb), JHEP **05**, 030 (2017), arXiv: 1701.07873[hep-ex]
[4] R. Aaij *et al.* (LHCb), Phys. Rev. Lett. **118**, 182001 (2017), arXiv: 1703.04639[hep-ex]
[5] R. Aaij *et al.* (LHCb), Phys. Rev. Lett. **124**, 222001 (2020), arXiv: 2003.13649[hep-ex]
[6] R. Aaij *et al.* (LHCb), Phys. Rev. Lett. **119**, 112001 (2017), arXiv: 1707.01621[hep-ex]
[7] R. Aaij *et al.* (LHCb), Phys. Rev. Lett. **121**, 162002 (2018), arXiv: 1807.01919[hep-ex]
[8] R. Aaij, A. S. W. Abdelmotteleb, C. Abellán Beteta, *et al.* (LHCb), JHEP **05**, 038 (2022), arXiv: 2202.05648[hep-ex]
[9] G. S. Abrams *et al.*, Phys. Rev. Lett. **44**, 10 (1980)
[10] Y. Q. Chen and S. Z. Wu, JHEP **08**, 144 (2011), arXiv: 1106.0193[hep-ph]
[11] W. Wang and J. Xu, Phys. Rev. D **97**, 093007 (2018), arXiv: 1803.01476[hep-ph]
[12] B. Silvestre-Brac, Few Body Syst. **20**, 1 (1996)
[13] W. Roberts and M. Pervin, Int. J. Mod. Phys. A **23**, 2817 (2008), arXiv: 0711.2492[nucl-th]
[14] J. Vijande, A. Valcarce, and H. Garcilazo, Phys. Rev. D **91**, 054011 (2015), arXiv: 1507.03735[hep-ph]
[15] G. Yang, J. Ping, P. G. Ortega *et al.*, Chin. Phys. C **44**, 023102 (2020), arXiv: 1904.10166[hep-ph]
[16] M. S. Liu, Q. F. Lü, and X. H. Zhong, Phys. Rev. D **101**, 074031 (2020), arXiv: 1912.11805[hep-ph]
[17] Z. Shah and A. K. Rai, Eur. Phys. J. A **53**, 195 (2017)
[18] B. Patel, A. Majethiya, and P. C. Vinodkumar, Pramana **72**, 679 (2009), arXiv: 0808.2880[hep-ph]
[19] J. R. Zhang and M. Q. Huang, Phys. Lett. B **674**, 28 (2009), arXiv: 0902.3297[hep-ph]
[20] Z. G. Wang, Commun. Theor. Phys. **58**, 723 (2012), arXiv: 1112.2274[hep-ph]
[21] T. M. Aliev, K. Azizi, and M. Savcı, J. Phys. G **41**, 065003 (2014), arXiv: 1404.2091[hep-ph]
[22] H. Sanchis-Alepuz, R. Alkofer, G. Eichmann, and R. Williams, PoS **QCD-TNT-II**, 041 (2011), arXiv: 1112.3214[hep-ph]
[23] M. Radin, Sh. Babaghodrat, and M. Monemzadeh, Phys. Rev. D **90**, 047701 (2014)
[24] S. x. Qin, C. D. Roberts, and S. M. Schmidt, Few Body Syst. **60**, 26 (2019), arXiv: 1902.00026[nucl-th]
[25] K. Thakkar, A. Majethiya, and P. C. Vinodkumar, Eur. Phys. J. Plus **131**, 339 (2016), arXiv: 1609.05444[hep-ph]
[26] P. L. Yin, C. Chen, G. Krein *et al.*, Phys. Rev. D **100**, 034008 (2019), arXiv: 1903.00160[nucl-th]
[27] Y. Jia, JHEP **10**, 073 (2006), arXiv: hep-ph/0607290
[28] J. M. Flynn, E. Hernandez, and J. Nieves, Phys. Rev. D **85**,

014012 (2012), arXiv: 1110.2962[hep-ph]
[29] A. Bernotas and V. Simonis, Lith. J. Phys. **49**, 19 (2009), arXiv: 0808.1220[hep-ph]
[30] P. Hasenfratz, R. R. Horgan, J. Kuti *et al*., Phys. Lett. B **94**, 401 (1980)
[31] K.-W. Wei, B. Chen, and X. H. Guo, Phys. Rev. D **92**, 076008 (2015), arXiv: 1503.05184[hep-ph]
[32] S. Migura, D. Merten, B. Metsch *et al*., Eur. Phys. J. A **28**, 41 (2006), arXiv: hep-ph/0602153
[33] T. W. Chiu and T. H. Hsieh, Nucl. Phys. A **755**, 471 (2005), arXiv: hep-lat/0501021
[34] R. A. Briceno, H. W. Lin, and D. R. Bolton, Phys. Rev. D **86**, 094504 (2012), arXiv: 1207.3536[hep-lat]
[35] Y. Namekawa *et al*. (PACS-CS), Phys. Rev. D **87**, 094512 (2013), arXiv: 1301.4743[hep-lat]
[36] M. Padmanath, R. G. Edwards, N. Mathur *et al*., Phys. Rev. D **90**, 074504 (2014), arXiv: 1307.7022[hep-lat]
[37] Z. S. Brown, W. Detmold, S. Meinel *et al*., Phys. Rev. D **90**, 094507 (2014), arXiv: 1409.0497[hep-lat]
[38] K. U. Can, G. Erkol, M. Oka *et al*., Phys. Rev. D **92**, 114515 (2015), arXiv: 1508.03048[hep-lat]
[39] C. Alexandrou, V. Drach, K. Jansen *et al*., Phys. Rev. D **90**, 074501 (2014), arXiv: 1406.4310[hep-lat]
[40] H. Bahtiyar, K. U. Can, G. Erkol *et al*., Phys. Rev. D **102**, 054513 (2020)
[41] C. Alexandrou and C. Kallidonis, Phys. Rev. D **96**, 034511 (2017), arXiv: 1704.02647[hep-lat]
[42] C. Alexandrou, J. Carbonell, D. Christaras *et al*., Phys. Rev. D **86**, 114501 (2012), arXiv: 1205.6856[hep-lat]
[43] S. Durr, G. Koutsou, and T. Lippert, Phys. Rev. D **86**, 114514 (2012), arXiv: 1208.6270[hep-lat]
[44] Y. C. Chen and T. W. Chiu (TWQCD), Phys. Lett. B **767**, 193 (2017), arXiv: 1701.02581[hep-lat]
[45] X. D. J, Phys. Rev. Lett. **74**, 1071 (1995), arXiv: hep-ph/9410274
[46] Y. B. Yang, Y. Chen, T. Draper *et al*., Phys. Rev. D **91**, 074516 (2015), arXiv: 1405.4440
[47] Y. B. Yang, J. Liang, Y. J. Bi *et al*., Phys. Rev. Lett. **121**, 212001 (2018), arXiv: 1808.08677[hep-lat]
[48] W. Sun, Y. Chen, P. Sun *et al*., Phys. Rev. D **103**, 094503 (2021), arXiv: 2012.06228
[49] R. Horsley *et al*. (QCDSF, UKQCD), Phys. Lett. B **714**, 312 (2012), arXiv: 1205.6410[hep-lat]
[50] M. A. Shifman, A. I. Vainshtein, and V. I. Zakharov, Phys. Lett. B **78**, 443 (1978)
[51] J. Liang, W. Sun, Y. Chen *et al*., Chin. Phys. C **40**, 41001 (2016), arXiv: 1511.04294
[52] C. Alexandrou *et al*. (European Twisted Mass), Phys. Rev. D **78**, 014509 (2008), arXiv: 0803.3190[hep-lat]
[53] Y. Aoki *et al*. (RBC, UKQCD), Phys. Rev. D **83**, 074508 (2011), arXiv: 1011.0892[hep-lat]
[54] R. D. Mawhinney (RBC, UKQCD), 2+*1 flavor domain wall fermion qcd lattices: Ensemble production and (some) properties*, (2019), arXiv: 1912.13150[hep-lat]
[55] Z. Liu *et al*. (chiQCD), Phys. Rev. D **90**, 034505 (2014), arXiv: 1312.7628[hep-lat]
[56] J. Liang, Y. Chen, M. Gong *et al*., Phys. Rev. D **89**, 094507 (2014), arXiv: 1310.3532[hep-lat]
[57] C. C. Chang *et al*., Nature **558**, 91 (2018), arXiv: 1805.12130[hep-lat]
[58] C. Bouchard, C. C. Chang, T. Kurth *et al*., Phys. Rev. D **96**, 014504 (2017), arXiv: 1612.06963[hep-lat]
[59] N. S. Dhindsa, D. Chakraborty, A. Radhakrishnan *et al*., *Precise study of triply charmed baryons* Ω_{ccc}, (2024), arXiv: 2411.12729[hep-lat]
[60] B. Hu, X. Jiang, K. F. Liu *et al*., *Trace anomaly contributions to baryon masses from Lattice QCD*, (2024), arXiv: 2411.18402[hep-lat]
[61] Y. Lyu, H. Tong, T. Sugiura *et al*., Phys. Rev. Lett. **127**, 072003 (2021), arXiv: 2102.00181[hep-lat]
[62] Y. Maezawa and P. Petreczky, Phys. Rev. D **94**, 034507 (2016), arXiv: 1606.08798[hep-lat]
[63] Y. Bi *et al*. (χQCD), Phys. Rev. D **108**, 054506 (2023), arXiv: 2302.01659[hep-lat]
[64] F. He *et al*. (χQCD), Phys. Rev. D **106**, 114506 (2022), arXiv: 2204.09246[hep-lat]
[65] H. J. Rothe, Phys. Lett. B **355**, 260 (1995), arXiv: hep-lat/9504012
[66] K. F. Liu, Phys. Rev. D **104**, 076010 (2021), arXiv: 2103.15768[hep-ph]